Original Article

High yield and efficient expression and purification of the human 5-HT$_{3A}$ receptor

Zhong-shan WU[1, 2], Zhi-cheng CUI[3], Hao CHENG[2], Chen FAN[3], Karsten MELCHER[4], Yi JIANG[2], Cheng-hai ZHANG[2], Hua-liang JIANG[5], Yao CONG[2], Qian LIU[1, *], H Eric XU[2, 4, *]

[1]Britton Chance Center for Biomedical Photonics, Wuhan National Laboratory for Optoelectronics, Huazhong University of Science and Technology, Wuhan 430074, China; [2]VARI-SIMM Center, Center for Structure and Function of Drug Targets, CAS-Key Laboratory of Receptor Research, Shanghai Institute of Materia Medica, Chinese Academy of Sciences, Shanghai 201203, China; [3]National Center for Protein Science Shanghai, State Key Laboratory of Molecular Biology, Institute of Biochemistry and Cell Biology, Shanghai Institutes for Biological Sciences, Chinese Academy of Sciences, Shanghai 201210, China; [4]Laboratory of Structural Sciences, Van Andel Research Institute, Grand Rapids, MI 49503, USA; [5]State Key Laboratory of Drug Research, Shanghai Institute of Materia Medica, Chinese Academy of Sciences, Shanghai 201203, China

Aim: To establish a method for efficient expression and purification of the human serotonin type 3A receptor (5-HT$_{3A}$) that is suitable for structural studies.

Methods: Codon-optimized cDNA of human 5-HT$_{3A}$ was inserted into a modified BacMam vector, which contained an IgG leader sequence, an 8×His tag linked with two-Maltose Binding Proteins (MBP), and a TEV protease cleavage site. The BacMam construct was used to generate baculoviruses for expression of 5-HT$_{3A}$ in HEK293F cells. The proteins were solubilized from the membrane with the detergent $C_{12}E_9$, and purified using MBP affinity chromatography. The affinity tag was removed by TEV protease treatment and immobilized metal ion affinity chromatography. The receptors were further purified by size-exclusion chromatography (SEC). Western blot and SDS-PAGE were used to detect 5-HT$_{3A}$ during purification. The purified receptor was used in crystallization and analyzed with negative stain electron microscopy (EM).

Results: The BacMam system yielded 0.5 milligram of the human 5-HT$_{3A}$ receptor per liter of cells. MBP affinity purification resulted in good yields with high purity and homogeneity. SEC profiles indicated that the purified receptors were pentameric. No protein crystals were obtained; however, a reconstructed 3D density map generated from the negative stain EM data fitted well with the mouse 5-HT$_{3A}$ structure.

Conclusion: With the BacMam system, robust expression of the human 5-HT$_{3A}$ receptor is obtained, which is monodisperse, therefore enabling 3D reconstruction of an EM map. This method is suitable for high-throughput screening of different constructs, thus facilitating structural and biochemical studies of the 5-HT$_{3A}$ receptor.

Keywords: human 5-HT$_{3A}$ receptor; BacMam; expression and purification; negative stain electron microscopy; receptor structure

Introduction

The physiological function of neuronal cells is primarily based on the conversion between chemical and electrical signals. Transmembrane receptors of the Cys-loop receptor (CLR) family play important roles in mediating rapid signal transduction between neuronal cells by converting chemical signals into electrical signals. Conversely, voltage-dependent calcium channels that regulate the vesicular release of neurotransmitters convert electrical signals into chemical signals. CLRs are responsible for fast excitatory and inhibitory transmission in the peripheral and central nervous systems[1]. CLRs are composed of five protein subunits that form a pentameric arrangement around a central ion-conducting pore. Each subunit consists of four parts: (1) a large extracellular ligand-binding domain (ECD), (2) three highly conserved transmembrane helices that allow ions to pass across the membrane, (3) an intracellular loop domain (ICD) of variable size and amino acid sequence, and (4) a fourth transmembrane helix with a relatively short and variable extracellular C-terminus
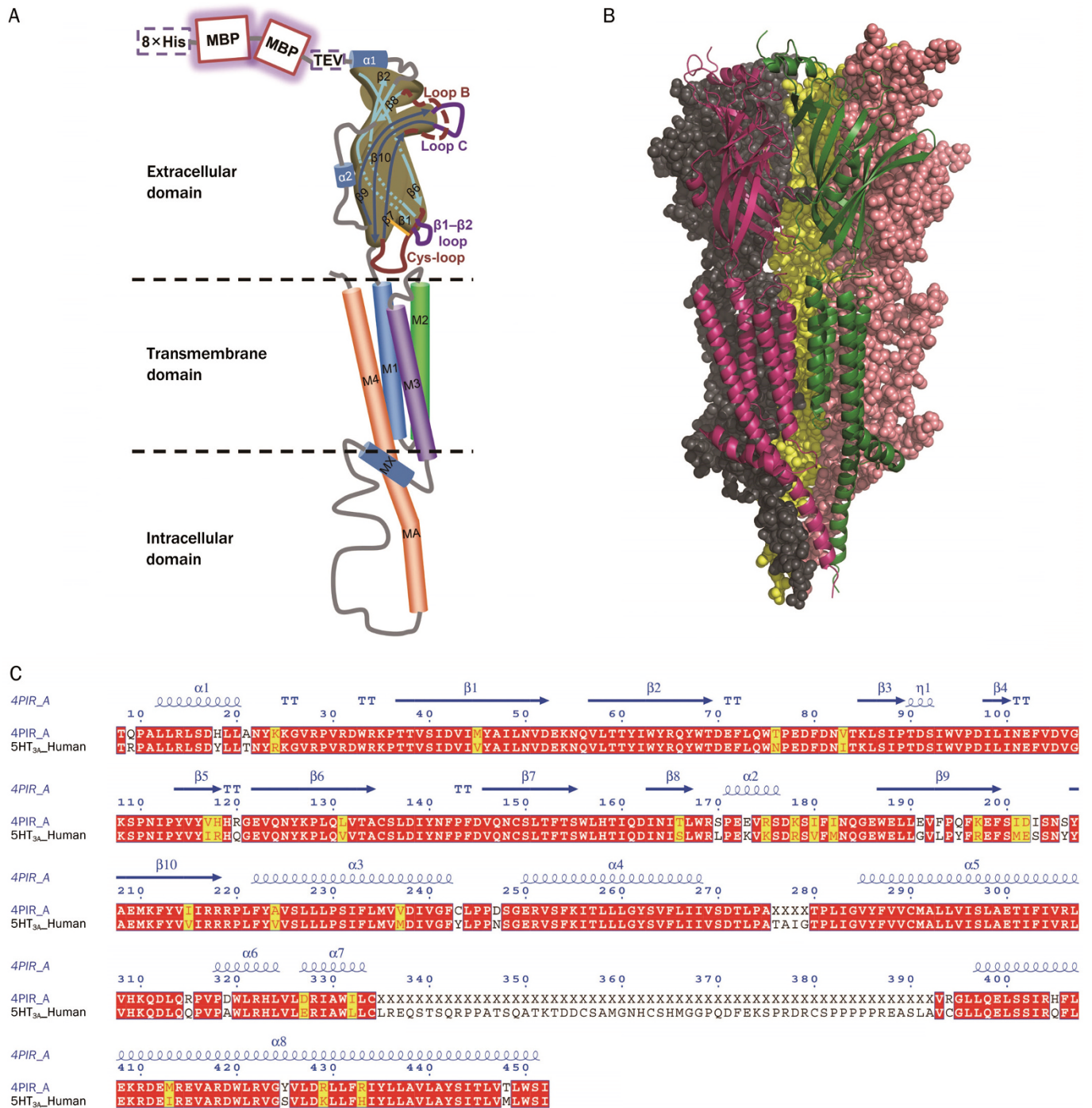
(Figure 1). The ECD harbors a signature sequence of 13 residues flanked by two cysteines, which bond covalently to form a closed loop between the binding site and the channel domain[2]. The ICD is a major determinant of channel

Figure 1. Topology of the 5-HT$_{3A}$ receptor. (A) The domain arrangement of 5HT$_{3A}$ is shown for a single subunit, including the β-folded extracellular domain, the α-helical transmembrane domain, and the partially structured intracellular domain. Helices are shown as cylinders, arrows represent β-strands with arrow heads pointing toward their C-termini, and lines without arrow heads represent unstructured loops. (B) The X-ray structure of the mouse 5-HT$_{3A}$ receptor (PDB: 4PIR) consists of five identical subunits, two of which are shown in cartoon presentation and three in sphere presentation. The ion channel lined by M2 extends along the central five-fold symmetry axis. (C) Sequence alignment of the human and mouse 5-HT$_3$ subunits. 4PIR_A stands for Chain A of the pentameric mouse 5-HT$_3$ receptor structure deposited in the PDB. Residues with red and yellow background indicate identical and similar amino acids, respectively, while residues without background indicate amino acids that differ between human and mouse 5-HT$_{3A}$. Residue numbers and secondary structure annotation are based on the crystal structure (4PIR).

conductance[3, 4] and contains additional helical structures in the 5-HT$_{3A}$ receptor and neuron-type acetylcholine receptor (nAChR). The Torpedo nAChR EM structure shows an intracellular amphiphatic helix (MA helix)[5] and the recent crystal structure of the mouse 5-HT$_{3A}$ reveals an additional helix, MX, in the ICD (Figure 1)[6].

CLRs belong to the ligand gated ion channel superfamily and can be further subdivided into cation- and anion-selective channels, corresponding to excitatory receptors activated by acetylcholine (ACh) or serotonin (5-hydroxytryptamine or 5-HT), and inhibitory receptors activated by GABA (γ-aminobutyric acid) or glycine[2]. Within the CLR family, the serotonin 5-HT$_3$ receptor and nicotinic acetylcholine receptor are the most closely related by homology. Currently, five different human 5-HT$_3$ subunits are known: 5-HT$_{3A}$ through 5-HT$_{3E}$. Of these five subunits, only 5-HT$_{3A}$ forms homopentameric ion channels[7], thus being the simplest subject for expression and structural study.

The serotonin 5-HT$_3$ receptor plays a role in emesis, memory, cognition, pain reception, sensory processing, motor neuron activity and substance addiction, and also regulates intestinal motility and secretion[8, 9]. Clinically, 5-HT3 receptor ligands are powerful therapeutic agents for the control and treatment of drug and alcohol dependence, schizophrenia, anxiety, cognitive dysfunction, and chemotherapy-induced and post-operative nausea and vomiting[10-13].

Serotonin- and granisetron-bound structures of 5-HT Binding Protein (5-HTBP) has revealed several important residues involved in ligand binding[14], and the recently determined crystal structure of a nanobody-bound mouse 5-HT$_{3A}$ receptor has afforded a detailed atomic map of 5-HT$_{3A}$ receptor and provided structural evidence for channel gate and ion selectivity[6]. However, molecular mechanisms that describe how the ligands bind, the conformational transitions between closed (rest) and open (active) channel states, the ion selectivity and the single-channel conductance determinants, are still not fully understood. High-efficiency large-scale production of recombinant receptors is required to obtain high-resolution structures of different states of 5-HT$_{3A}$ receptors.

The 5-HT$_{3A}$ receptor was first cloned in 1991[15], and its heterologous overexpression and purification was first reported in 1995[16]. Since 1995, extensive efforts have been made to express and purify 5-HT$_3$ receptors. The Semliki Forest Virus (SFV) expression system yields high expression of recombinant 5-HT$_3$ receptors, which can be scaled up to bioreactor scale. Previous studies have shown $C_{12}E_9$ was the most suitable detergent for solubilization of 5-HT$_{3A}$ receptor[17, 18]. A fusion protein of P9 protein, a major envelope protein of bacteriophage phi6, and 5-HT$_{3A}$ was highly expressed in the membrane fraction of *Escherichia coli*[19]. Inducible, stable expression in HEK293 suspension cells resulted in high yields of the mouse 5-HT$_3$ receptor[20].

In addition to high yields, affinity purification, proteolysis treatment and nanobody binding led to the determination of the crystal structure of the mouse 5-HT$_3$[6]. However, these efforts have several shortcomings, such as the feasibility at the lab-scale, time required, protein quality and throughput. Generation of a recombinant virus is complicated and time consuming for the SFV expression system. The purified P9 fusion 5-HT$_{3A}$ from *E coli* is a mixture of oligomers and is therefore unsuitable for structural studies. Establishing stable cell lines is time consuming and cannot be used for high throughput screening of different constructs for protein engineering studies. Here, we demonstrate high-efficiency milligram-scale expression and purification of the human 5-HT$_{3A}$ receptor using a modified BacMam expression. The purified receptor forms a uniform pentameric complex of five identical subunits and provides a basis for future high-resolution structure studies of the 5-HT$_{3A}$ receptor using X-ray crystallography or single particle cryo-EM analysis.

Materials and methods

Materials

Restriction enzymes were purchased from Fermentas (Burlington, ON, Canada), DNA polymerase was purchased from New England Biolabs (Ipswich, MA, USA). DMEM/HIGH GLUCOSE cell medium and FBS were from Hyclone (Logan, UT, USA) and trypsin-EDTA, PBS, GlutaMAX, HEPES, and sodium pyruvate were from Gibco(Grand Island, NY, USA). $C_{12}E_9$ was purchased from Sigma-Aldrich (St Louis, MO, USA). Molecular weight markers for SDS-PAGE were from Thermo Fisher Scientific(Waltham, MA, USA).

Cloning

To direct membrane protein expression in mammalian cells after baculovirus transduction[21], a BacMam vector was constructed from pFastBac1 (Invitrogen, Cergy Pontoise, France), by replacing the polyhedron promoter (P_{PH}) with the CMV promoter (P_{CMV}) and inserting a N-terminal fusion cassette consisting of a Kozak consensus sequence-IgG leader-8×His-MBP-MBP-TEV protease cleavage site). Codon-optimized human 5-HT$_{3A}$ (NCBI accession number: P46098.1) cDNA lacking the predicted signal peptide coding region (N-terminal residues 1 approximately 23) was synthesized (GENEWIZ) with the flanking restriction sites *Nhe*I at the 5' end and *Not*I at the 3' end. This fragment was cloned downstream of the Tetracycline Response Element (TRE)-driven expression cassette of a modified BacMam vector, consisting of an IgG leader sequence (MGWSCIILFLVATATGVHSE) followed by an 8×His tag, a tandem MBP tag, a linker-flanked TEV cleavage sequence (GSAENLYFQGGSA), and *Nhe*I and *Not*I restriction sites for insertion of the 5-HT$_{3A}$ cDNA. For the fusion protein with green fluorescence protein (GFP), the MBP tag was replaced with the cDNA of GFP upstream of the TEV cleavage site ahead of the human 5-HT$_{3A}$ receptor. The components of the expression cassette were introduced using standard PCR reactions followed by restriction digestions and ligations.

Virus production and amplification

High titer recombinant baculovirus (>10^8 viral particles per mL) was obtained using the Bac-to-Bac Baculovirus Expression System (Invitrogen). Briefly, the BacMam constructs

were transformed into DH10BAC competent cells, followed by the standard blue/white α-complementation screen. Positive colonies were picked and grown in 5 mL of LB medium with 50 μg/mL kanamycin, 7 μg/mL gentamicin and 10 μg/mL tetracycline at 37 °C overnight with shaking at 200 r/min. The cells were collected for bacmid extraction following the standard protocol (Invitrogen). Then, 5 μg of extracted bacmid DNA were transfected into 2.5 mL of Sf9 cells at a cell density of 2×10^6 cells/mL using 2 μL of X-tremeGene Transfection Reagent (Roche, Basel, Switzerland) and 100 μL of OPTI-MEM medium (Gibco). The Sf9 cell suspensions were incubated in 24-deep-well plates at 27 °C with shaking at 300 r/min. P0 viral stocks were isolated after 4 d and used to produce high titer baculovirus ($>10^9$ viral particles per mL) stocks P1 and P2 with Sf9 cells. Viral titers were determined by flow cytometric methods by staining cells with gp64-PE (Expression Systems, Davis, CA, USA).

Mammalian cell maintenance and protein expression

The HEK293F (FreeStyle293F cells, Invitrogen) cell line was maintained at 37 °C in a 70% humidity and 5% CO_2 atmosphere in tissue culture-treated flasks containing DMEM/HIGH GLUCOSE medium with *L*-glutamine and 10% FBS. When cells reached 80%–90% confluence they were detached by trypsinization and re-seeded at a 4–6-fold dilution into fresh medium. When needed, the cells were seeded in 12-well plates for small-scale protein expression. Cells were collected 24 h after baculovirus transduction at an MOI of 50 and doxycycline induction, typically at final concentration of 1 μg/mL.

Adherent HEK293F cells were seeded in 10 cm diameter dishes. When cells reached 90%–100% confluence, the medium was removed and cells were resuspended in 50 mL warm CDM4HEK293 medium with 4 mmol/L GlutaMax, 10 mmol/L HEPES and 1 mmol/L sodium pyruvate. Cells were then transferred to 250 mL cell culture flasks and grown at 37 °C in a 70% humidity/5% CO_2 atmosphere with shaking at 125 r/min. When cells reached a density of 3×10^6 cells/mL, they were diluted 3-fold with the aforementioned suspension medium. Finally, suspension HEK293F cells were maintained in 2.8-L flasks at a maximal volume of 500 mL for protein expression.

For large-scale expression in mammalian cells, suspension HEK293F cells at a density of 2×10^6 cells/mL were transduced with P2 virus with an MOI of 50. Cells were induced with 1 μg/mL doxycycline for protein expression and were harvested by centrifugation at $2000 \times g$ for 20 min 24 h post induction. These samples were stored at -80 °C until use.

Western blot

Proteins were expressed as described above, and cell pellets were solubilized in lysis reagent (CelLytic™ M, Sigma) supplemented with 1 mmol/L PMSF and then centrifuged at $16\,100 \times g$ for 30 min. The supernatant was mixed with SDS loading buffer and subjected to SDS-PAGE (8%) in the presence and absence of 150 mmol/L β-mercaptoethanol. Then, the proteins were transferred to PVDF membranes. The membranes were blocked with 5% milk in TBST (20 mmol/L Tris-HCl pH 8.0, 150 mmol/L NaCl and 0.05% Tween-20), and then incubated with mouse monoclonal antibodies (made in the institute antibody facility) against MBP (Maltose Binding Protein), followed by HRP-conjugated anti-mouse antibodies in 5% milk dissolved in TBST. Protein bands were detected by incubation with SuperSignal West Pico Chemiluminescent Substrate (Thermo Scientific), and imaged using the Chemi-Doc™ XRS+system (BIO-RAD, Hercules, CA, USA).

Fluorescence microscopy

Adherent HEK293F cells were grown in routine medium and the GFP/human 5-HT$_3$ receptor fusion was expressed by transducing the corresponding recombinant baculovirus with an MOI of 50, 24 h before measuring fluorescence. Fluorescence images were recorded on a customized, wide-field epifluorescence microscope (Nikon TE2000, Mississauga, ON, Canada) using the appropriate excitation and emission filters.

Membrane preparation and solubilization

All steps were performed at 4 °C unless indicated otherwise. Frozen cell pellets were resuspended in a hypotonic buffer containing 10 mmol/L HEPES (pH 7.4), 10 mmol/L $MgCl_2$, 20 mmol/L KCl, 1 mmol/L EDTA and complete protease inhibitor cocktail (Roche). The cell suspension was homogenized with a Dounce homogenizer, and the homogenate was centrifuged at $65\,000 \times g$ for 45 min. Extensive washing of the raw membranes was performed by three consecutive cycles of centrifugation in hypotonic buffer, followed by resuspension in a highly osmotic buffer containing 1.0 mol/L NaCl, 50 mmol/L Tris-HCl (pH 7.4). Therefore, the soluble and membrane associated proteins were separated from integral transmembrane proteins. Washed membranes were resuspended into solubilization buffer containing 150 mmol/L NaCl, 50 mmol/L Tris-HCl (pH 7.4), 4 mmol/L $C_{12}E_9$ and complete protease inhibitor cocktail, and incubated for 4 h with gentle agitation. The supernatant was isolated by centrifugation at $110\,000 \times g$ for 1 h and used in subsequent purification steps.

Affinity purification and tag removal

The supernatant was incubated with amylose resin (New England Biolabs) equilibrated in buffer containing 150 mmol/L NaCl, 50 mmol/L Tris-HCl (pH 7.4), 0.2 mmol/L $C_{12}E_9$ (Buffer A) overnight at 4 °C. Typically, 2 mL of resin per 1 L of original culture volume was used. After binding, the resin was washed with 8–10 column volumes of Buffer A, and eluted with 3 column volumes of Buffer A supplemented with 20 mmol/L maltose. Purified 5-HT$_{3A}$ receptor was then incubated at 4 °C overnight in the presence of Ni-NTA-purified recombinant 6×His-TEV protease. Typically 1 μg of TEV protease per 3 μg of receptor was used. Nickel-chelating resin (GE Healthcare) was incubated at 4 °C for 1 h in the presence of 25 mmol/L imidazole to remove TEV protease and cleaved protein tag. The untagged receptor was collected in the flow-through. Protein purity and dispersity was assessed by SDS-PAGE and analytical size-exclusion chromatography (HPLC,

Agilent Technologies, Santa Clara, CA, USA).

Size-exclusion chromatography

The receptor was concentrated to approximately 5 mg/mL using a 100 kDa MWCO spin filter (Millipore, Billerica, MA, USA) and loaded onto a Superose 6 10/300 GL gelfiltration column (GE Healthcare) equilibrated in Buffer A, at flow rate of 0.5 mL/min in an AKTA FPLC (GE).

Amphipol exchange and detergent removal

Untagged 5-HT$_{3A}$ receptor was mixed with amphipols at a 1:3 (*w/w*) ratio with gentle agitation at 4 °C for 4 h. Detergent was removed through incubation with Bio-Beads SM-2 (BIO-RAD) at 4 °C overnight. Typically, 15 mg of Bio-Beads per 1 mL channel/detergent/amphipols mixture were used. Bio-Beads were then removed by passing through a disposable polyprep column. The eluent was cleared by centrifugation before further separation on a Superdex 200 10/300 GL or a Superose 6 10/300 GL gelfiltration column (GE Healthcare) in buffer composed of 150 mmol/L NaCl, 20 mmol/L HEPES, pH 7.4.

Negative stain EM

Negative stain EM was prepared by applying 5 µL of amphipol-exchanged 5-HT$_{3A}$ at a concentration of approximately 25 µg/mL to a glow-discharged 400 mesh continuous carbon grid (Beijing Zhongjingkeyi Technology Co, Ltd, Beijing, China), followed by staining with 0.75% (*w/v*) uranyl formate. Grids were transferred to a Tecnai G2 F20 TWIN transmission electron microscope (FEI Company, USA) equipped with a field-emission gun operated at 200 kV. Images were recorded at 55 000× microscope magnification with a 4k×4k Eagle CCD camera (corresponding to a pixel size of 1.48 Å/pixel) with defocus ranging from -0.8 to -1.2 µm.

Image processing and 3D reconstruction

The EM image processing was carried out in EMAN2 single particle analysis software package[22]. Using the e2boxer.py program, 5245 particles were boxed out for human 5-HT$_{3A}$. Reference-free 2D analysis was performed utilizing e2refine2d.py program. These class-averages were then used to generate an initial model by e2initialmodel.py. The following refinement was carried out using e2refine_easy.py with imposed 5-fold symmetry. The resolution was estimated at 27 Å using the 0.5 FSC criteria.

UCSF Chimera[23] was used to render the EM density map together with the X-ray model. Here, the fit in map module in Chimera was used for rigid-body fitting of the X-ray model into the EM density map.

Results

Membrane expression of the human 5-HT$_{3A}$ receptor

To screen the expression of the human 5-HT$_{3A}$, we generated DNA constructs containing the human IgG leader sequence, a poly-histidine tag followed by a tandem MBP purification tag, a TEV protease cleavage site, and the wild type or mutant serotonin 5-HT$_{3A}$. In some cases, a GFP tag was engineered at

the N-terminal of 5-HT$_{3A}$. These constructs were inserted into a modified BacMam vector to generate recombinant baculoviruses as described in the Methods section of this study. For small-scale protein expression, adherent HEK293F cells were grown at 37 °C in tissue culture-treated flasks or 12-well plates and transduced with baculoviruses when the cells reached 80% confluence. For large-scale protein expression, HEK293F suspension cells grown at 37 °C in an orbital shaker were transduced with baculoviruses when the cell density reached approximately 2×10^6 cells per mL. Cells were harvested 24 h after transduction for protein purification or identification.

HEK293F cells infected with recombinant baculovirus displayed robust plasma membrane expression of the MBP-fused 5-HT$_{3A}$ as detected by an anti-MBP antibody (Figure 2A). The constructs that contained a GFP tag showed surface expression, as observed by fluorescence microscopy (Figure 2B). Generally, we cultivated 2 L of cells in suspension per day, typically yielding 25 g of biomass and approximately 1 mg of pure pentameric protein.

Receptor solubilization

Our studies showed that the detergent C$_{12}$E$_9$ was well able to solubilize and stabilize the 5-HT$_3$ receptor[17]. Here, we used 4 mmol/L C$_{12}$E$_9$ during solubilization and 0.2 mmol/L during all subsequent purification steps. The detergent dodecyl maltoside (DDM), which is commonly used to solubilize G-protein coupled receptors (GPCR), was compared to C$_{12}$E$_9$ at a concentration of 0.5% (*w/v*) during solubilization and 0.02% during other steps. The results showed that both C$_{12}$E$_9$ and DDM solubilized the 5-HT$_3$ receptor very well (lanes 3 and 7, Figure 2C), but C$_{12}$E$_9$ behaved better in the affinity purification step (lane 5 *vs* 9, Figure 2C).

Affinity purification

Single-step affinity purification with amylose resin allowed the isolation of the receptor with high purity (Figure 2D). For our studies, two tandem MBP tags were used in an effort to increase the protein solubility and the binding affinity to the resin. As expected, less protein was detected in the flow-through when two MBP tags were used compared with a single MBP tag.

Size-exclusion chromatography and tag removal

The purified fusion receptor was digested with TEV protease and the double MBP tag coupled with an N-terminal 8×His tag was removed using a nickel column (Figure 2D-2E). In SDS-PAGE, the primary band migrated above the 50 kDa marker. However, the band was diffused due to complex glycosylation of the receptor. There were also contaminating proteins of approximately 85 kDa during all the purification steps, which were not detected by the anti-MBP antibody (Figure 2A and 2C–2E). A Superose 6 10/300 GL column was selected to separate the pentameric receptors because this column can separate proteins that are less than 1000 kDa. We observed peaks that correspond to the pentameric 5-HT$_{3A}$ receptor both before and after TEV cleavage of the tag (Figure 3). Based on
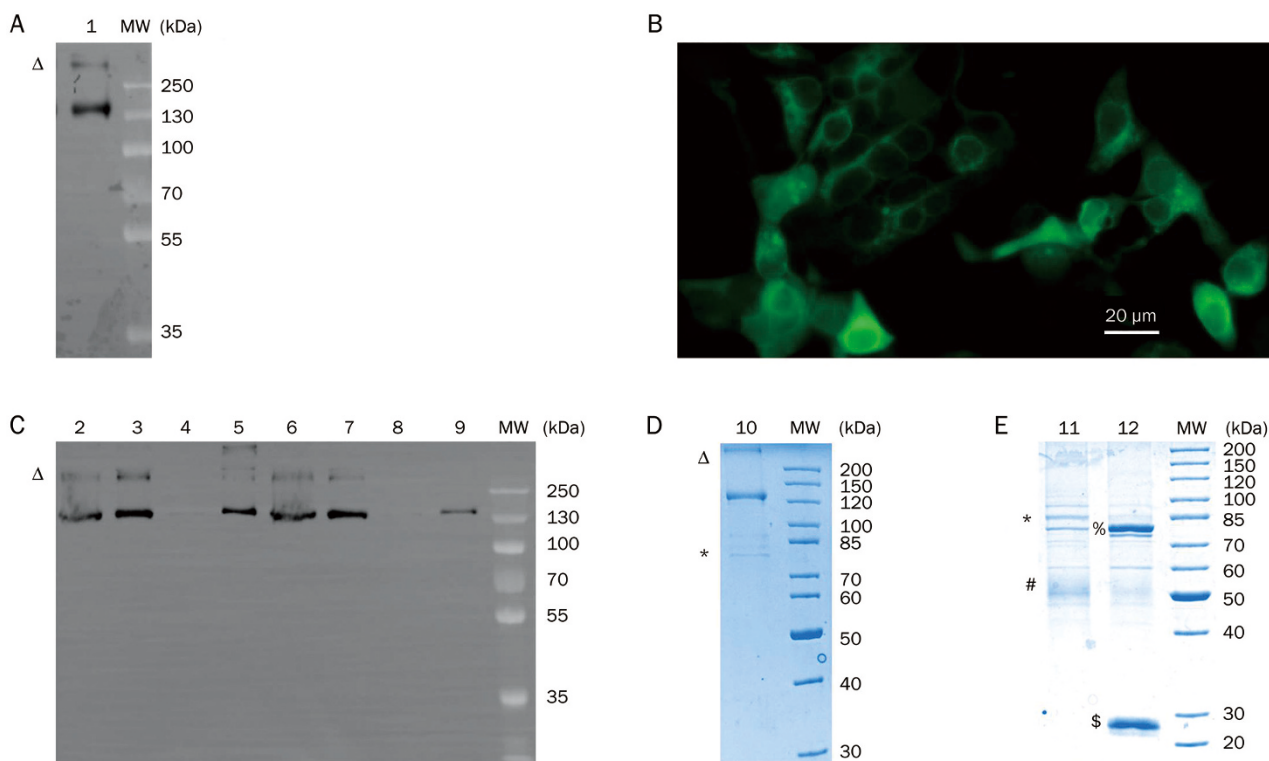
Figure 2. Expression of 5-HT$_3$ receptors. (A) Western blot of the 8×His-MBP-MBP-fused human 5-HT$_{3A}$ receptor expressed in adherent HEK293F cells. (B) Confocal images were obtained from the HEK293F cell line expressing GFP-fused human 5-HT$_{3A}$ receptor following recombinant baculovirus transduction. (C) Western blot of different samples during solubilization and purification with detergent C$_{12}$E$_9$ (lane 2–5) or DDM (lane 6–9): lane 2 and lane 6 contain total membranes, lane 3 and lane 7 contain solubilized proteins, lane 4 and lane 8 contain the flow-through fraction from MBP affinity purification, and lane 5 and lane 9 contain elution samples. (D) Coomassie brilliant blue-stained SDS-PAGE gel with elution fractions from the MBP column, the triangle sign (Δ) indicates oligomeric (probably dimer) H8-MBP-MBP-5-HT$_{3A}$ subunits (lane 10). (E) Removal of the 8×His-double MBP tag and the 6×His-TEV protease after TEV treatment is demonstrated by SDS-PAGE. After loading the TEV protease-treated eluate on a nickel column, the flow-through (lane 11) contained the receptor and contaminated proteins, while the elute fraction (lane 12) contained the double MBP tag and TEV protease. The asterisk (*) indicates contaminating proteins that could not be separated during purification, the number sign (#) indicates monomer 5-HT$_{3A}$, the percentage sign (%) indicates the double MBP tag, and the dollar sign ($) indicates TEV protease.
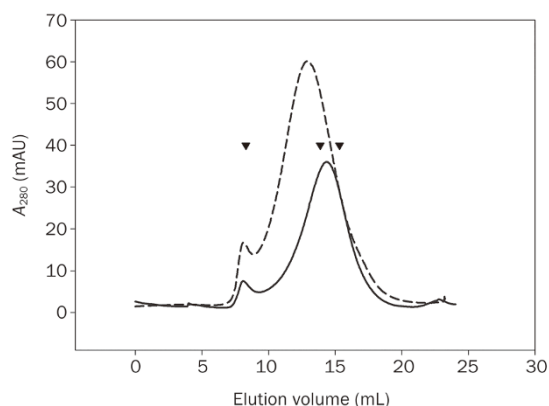
Figure 3. Size-exclusion chromatography (SEC) profiles of the human 5-HT$_3$ receptor at different steps of the purification on a Superose 6 10/300 GL column. The elution profile before (dash line) and after (solid line) TEV treatment is shown with the main peaks compatible with corresponding pentameric protein-detergent complexes. Inverted triangles indicate elution volumes of protein standards [from left to right, dextran blue [void volume], thyroglobulin (669 kDa), ferritin (440 kDa)].

the comparison with the protein standards profile, the peaks of the receptor before and after tag cleavage correspond to molecular masses greater than 669 kDa and between 440 kDa and 669 kDa, respectively. These estimated molecular masses of the receptor were approximated to the expected molecular masses for the pentameric protein-detergent complexes which were composed of a pentameric protein of approximately 5×130=650 kDa (with the tag) or 5×52=260 kDa (without the tag) with the additional mass of detergent micelle, which has an equivalent mass in the case of untagged receptor.

Negative stain EM and 3D reconstruction

The SEC peak fractions were concentrated to approximately 15 mg/mL and used for crystallization experiments. However, despite extensive screening efforts, we did not obtain any protein crystals. Therefore, we attempted cryo-EM technology as a means of structure analysis of ion channels, as successfully demonstrated for the structure determination of the ion channel TRPV1 at a near atomic resolution. Negative stain EM is an essential prerequisite to cryo-EM when evaluating the

quality of protein samples. Both DDM- and $C_{12}E_9$-solubilized 5-HT$_{3A}$ particles were roughly monodispersed as assessed by negative stain EM (Figure 4A, 4B), while amphipol-exchanged sample behaved better (Figure 4C) and enabled EM analysis and further 3D reconstruction (Figure 5A–5C). The resulting top view class-averages revealed the existence of 5-fold symmetry (Figure 5A and 5C).

The overall EM 3D density map fitted well with the recently determined X-ray structure of the mouse 5-HT$_{3A}$ receptor. Interestingly, the 5-HT$_{3A}$ receptor with the tag showed significantly more aggregate particles under the same condition, which may be due to the flexibility of the large MBP-MBP purification tag (Figure 4D). Upon fitting to the X-ray structure, our EM density map showed extra densities around the TMD and the ICD (Figure 5A), which may be attributed to amphipol molecules that surround the TMD and the missing part of intracellular loops in the 5-HT$_{3A}$ X-ray structure, respectively.

Discussion

Major progress has been made in structural studies of ligand-gated ion channels, including X-ray structures of recombinantly-expressed Gloeobacter Ligand-gated Ion Channel (GLIC), Erwinia Ligand-gated Ion Channel (ELIC), GluCl, and GABA β3 receptors[24–27]. The recent breakthrough structure of the mouse 5-HT$_{3A}$ receptor revealed part of the intracellular domain and provided the structural basis for understanding the gating mechanism of mammalian Cys-loop receptors at high resolution. However, key questions remain with regard to the open and closed states of the receptor as well as the intact structure of the ICD. Furthermore, the human 5-HT$_{3A}$ receptor is more clinically relevant than the mouse receptor and will ultimately be the target for drug binding. High and efficient expression and purification of the human 5-HT$_{3A}$ is the first step toward addressing these challenges.

Mammalian systems have been shown to be suitable for expression of mammalian proteins due to their ability to perform post-translational modifications, and their targeting and membrane insertion machineries that differ from other cell types. In this report, we demonstrated a new strategy for robust expression of the human 5-HT$_{3A}$ receptor in mammalian cells and verified that the yield is suitable for structural studies using X-ray crystallography and cryo-EM analysis. The recombinant baculoviruses can be rapidly amplified using the mature Bac-to-Bac system, obviating the need to generate
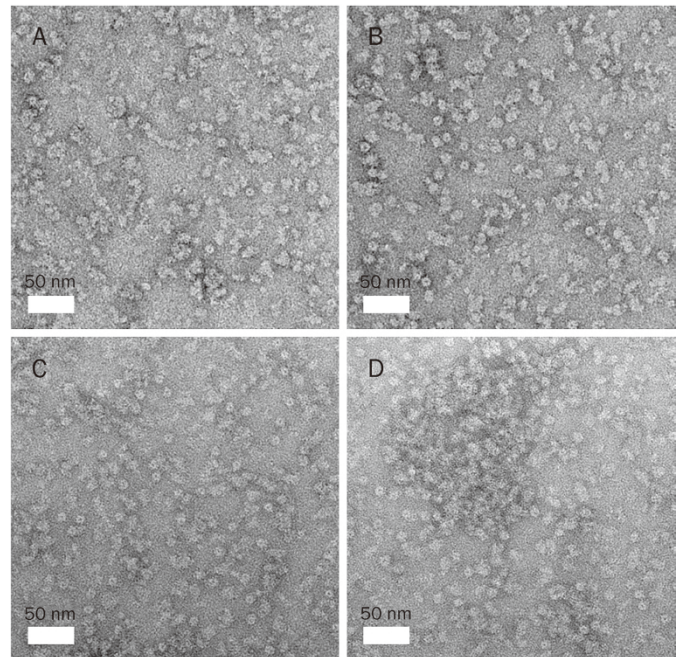

Figure 4. Electron micrographs of negative stain samples of the human 5-HT$_{3A}$ receptors at different steps of the purification. (A) The human 5-HT$_{3A}$ in DDM solution; (B) The human 5-HT$_{3A}$ in $C_{12}E_9$ solution; (C) The human 5-HT$_{3A}$ in amphipol solution; (D) 8×His-MBP-MBP-5-HT$_{3A}$ in amphipol solution.

stable cell lines and transfect large amounts of DNA into cells. HEK293F suspension cells can be kept at an appropriate cell density for more than 2 months; thus, it is possible to express one batch recombinant proteins every day. Indeed, most membrane protein structures were obtained from heavily engineered proteins, which require efficient expression systems. For example, for structural studies of GPCRs, fusion partners and thermo stability mutations were usually introduced into the receptors[28, 29]. In the case of the NMDA receptor, combinations of cross-linking and point mutations were introduced to stabilize the receptor for crystallization[30]. The advantages of the BacMam expression system allow high-throughput screening of different constructs that contain recombinant proteins. Compared with other systems investigated over the years (Table 1), our expression strategy provides an efficient way to produce an active human 5-HT$_{3A}$ receptor that is suitable for protein structure studies.

Table 1. Comparison between existing mammalian expression systems used for 5-HT$_{3A}$ receptor expression.

Mammalian expression system	Time cost			Money cost		
	Stable cell line preparation	Virus preparation	Protein expression	DNA/RNA preparation	Man-power	Medium
SFV system	–	Less than 1 week	16–18 h	*In-vitro* RNA, expensive	Very skilled, not much	Medium with FCS
BacMam system	–	1 week	24 h	Bacmid DNA, cheap	Skilled, not much	Serum-free medium
Stable cell line	3 months	–	48 h	Plasmid DNA, cheap	Skilled, much	Serum-free medium
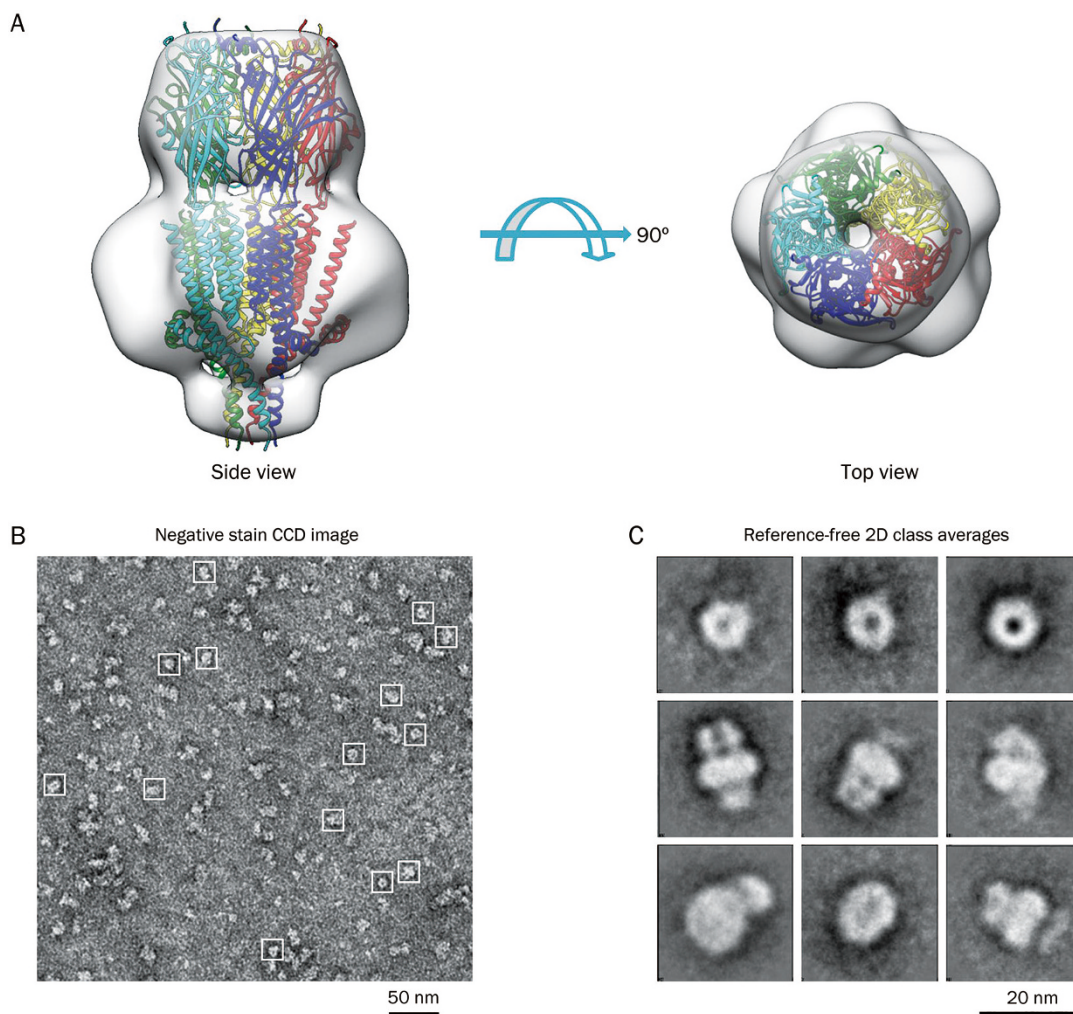
Figure 5. Fitting of the negative stain EM density map of the human 5-HT$_{3A}$ receptor with X-ray structure of the mouse 5-HT$_{3A}$ receptor. (A) The left panel shows the side view that is parallel to the plane of the membrane, and the right panel shows the extracellular view, which is perpendicular to the membrane (top view). (B) The EM map fits well with the X-ray structure, especially at the extracellular domain, while extra densities at the transmembrane domain and intracellular domain can be explained by bound amphipol molecules and unstructured intracellular loops, respectively. Typical negative stain CCD image of human 5-HT$_{3A}$. Representative particles are highlighted by white boxes. (C) Representative reference-free 2D class averages of human 5-HT$_{3A}$ showing the characteristic top and side view features.

Purified 5-HT$_{3A}$ functioned well in the presence of amphipol in negative stain EM, which revealed monodispersed pentameric complexes, consistent with the overall arrangement of ligand-gated ion channels. Our results indicate that our purified receptor might be suitable for single particle cryo-EM analysis. Recent cryo-EM structures of the TRPV1 ion channel in the apo- or ligand-bound states suggest that cryo-EM is particularly well-suited for determining the protein structure in multiple conformational states. The efficient method of expression and purification of 5-HT$_{3A}$ reported here provides a basis for future structural analysis of multiple conformational states of the receptor.

Acknowledgements

Author contribution

Zhong-shan WU designed and performed experiments and wrote the first draft of the paper; Zhi-cheng CUI, Chen FAN, and Yao CONG designed and performed EM experiments; Hao CHENG designed and performed experiments; Hua-liang JIANG and Qian LIU initiated collaborations and commented on the manuscript; Karsten MELCHER supervised experiments and commented on the manuscript; Yi JIANG and Cheng-hai ZHANG helped to design expression system

and experiments; H Eric XU conceived the project, supervised the work and wrote the manuscript with contribution from all authors.

References

1 Thompson AJ, Lester HA, Lummis SC. The structural basis of function in Cys-loop receptors. Q Rev Biophys 2010; 43: 449–99.

2 Sine SM, Engel AG. Recent advances in Cys-loop receptor structure and function. Nature 2006; 440: 448–55.

3 Kelley SP, Dunlop JI, Kirkness EF, Lambert JJ, Peters JA. A cytoplasmic region determines single-channel conductance in 5-HT$_3$ receptors. Nature 2003; 424: 321–4.

4 Peters JA, Cooper MA, Carland JE, Livesey MR, Hales TG, Lambert JJ. Novel structural determinants of single channel conductance and ion selectivity in 5-hydroxytryptamine type 3 and nicotinic acetylcholine receptors. J Physiol 2010; 588: 587–96.

5 Unwin N. Refined structure of the nicotinic acetylcholine receptor at 4A resolution. J Mol Biol 2005; 346: 967–89.

6 Hassaine G, Deluz C, Grasso L, Wyss R, Tol MB, Hovius R, *et al*. X-ray structure of the mouse serotonin 5-HT$_3$ receptor. Nature 2014; 512: 276–81.

7 Niesler B, Kapeller J, Hammer C, Rappold G. Serotonin type 3 receptor genes: HTR3A, B, C, D, E. Pharmacogenomics 2008; 9: 501–4.

8 Thompson AJ, Lummis SCR. The 5-HT$_3$ receptor as a therapeutic target. Expert Opinion on Therapeutic Targets 2007; 11: 527–40.

9 Walstab J, Rappold G, Niesler B. 5-HT(3) receptors: role in disease and target of drugs. Pharmacol Ther 2010; 128: 146–69.

10 Gregory RE, Ettinger DS. 5-HT$_3$ receptor antagonists for the prevention of chemotherapy-induced nausea and vomiting. A comparison of their pharmacology and clinical efficacy. Drugs 1998; 55: 173–89.

11 Greenshaw AJ. Behavioural pharmacology of 5-HT$_3$ receptor antagonists: a critical update on therapeutic potential. Trends Pharmacol Sci 1993; 14: 265–70.

12 Leeser J, Lip H. Prevention of postoperative nausea and vomiting using ondansetron, a new, selective, 5-HT$_3$ receptor antagonist. Anesth Analg 1991; 72: 751–5.

13 Grant KA. The role of 5-HT$_3$ receptors in drug dependence. Drug Alcohol Depend 1995; 38: 155–71.

14 Kesters D, Thompson AJ, Brams M, van Elk R, Spurny R, Geitmann M, *et al*. Structural basis of ligand recognition in 5-HT$_3$ receptors. EMBO Rep 2013; 14: 49–56.

15 Maricq AV, Peterson AS, Brake AJ, Myers RM, Julius D. Primary structure and functional expression of the 5HT$_3$ receptor, a serotonin-gated ion channel. Science 1991; 254: 432–7.

16 Green T, Stauffer KA, Lummis SC. Expression of recombinant homo-oligomeric 5-hydroxytryptamine3 receptors provides new insights into their maturation and structure. J Biol Chem 1995; 270: 6056–61.

17 Hovius R, Tairi AP, Blasey H, Bernard A, Lundstrom K, Vogel H. Characterization of a mouse serotonin 5-HT$_3$ receptor purified from mammalian cells. J Neurochem 1998; 70: 824–34.

18 Blasey HD, Brethon B, Hovius R, Vogel HH, Tairi AP, Lundstrom K, *et al*. Large scale transient 5-HT$_3$ receptor production with the *Semliki* forest virus expression system. Cytotechnology 2000; 32: 199–208.

19 Na JH, Shin J, Jung Y, Lim D, Shin YK, Yu YG. Bacterially expressed human serotonin receptor 3A is functionally reconstituted in proteoliposomes. Protein Expr Purif 2013; 88: 190–5.

20 Hassaine G, Deluz C, Tol MB, Li XD, Graff A, Vogel H, *et al*. Large scale expression and purification of the mouse 5-HT$_3$ receptor. Biochim Biophys Acta 2013; 1828: 2544–52.

21 Dukkipati A, Park HH, Waghray D, Fischer S, Garcia KC. BacMam system for high-level expression of recombinant soluble and membrane glycoproteins for structural studies. Protein Expr Purif 2008; 62: 160–70.

22 Tang G, Peng L, Baldwin PR, Mann DS, Jiang W, Rees I, *et al*. EMAN2: an extensible image processing suite for electron microscopy. J Struct Biol 2007; 157: 38–46.

23 Pettersen EF, Goddard TD, Huang CC, Couch GS, Greenblatt DM, Meng EC, *et al*. UCSF Chimera — a visualization system for exploratory research and analysis. J Comput Chem 2004; 25: 1605–12.

24 Miller PS, Aricescu AR. Crystal structure of a human GABA$_A$ receptor. Nature 2014; 512: 270–5.

25 Hibbs RE, Gouaux E. Principles of activation and permeation in an anion-selective Cys-loop receptor. Nature 2011; 474: 54–60.

26 Hilf RJ, Dutzler R. Structure of a potentially open state of a proton-activated pentameric ligand-gated ion channel. Nature 2009; 457: 115–8.

27 Hilf RJ, Dutzler R. X-ray structure of a prokaryotic pentameric ligand-gated ion channel. Nature 2008; 452: 375–9.

28 Tan Q, Zhu Y, Li J, Chen Z, Han GW, Kufareva I, *et al*. Structure of the CCR5 chemokine receptor-HIV entry inhibitor maraviroc complex. Science 2013; 341: 1387–90.

29 Wang C, Jiang Y, Ma JM, Wu HX, Wacker D, Katritch V, *et al*. Structural basis for molecular recognition at serotonin receptors. Science 2013; 340: 610–4.

30 Karakas E, Furukawa H. Crystal structure of a heterotetrameric NMDA receptor ion channel. Science 2014; 344: 992–7.